BEAMFORMING WITH EXTENDED CO-PRIME SENSOR ARRAYS

Kaushallya Adhikari⋆ *John R. Buck*⋆ *Kathleen E. Wage*†

⋆ {kadhikari,jbuck}@umassd.edu
Electrical and Computer Engineering Department
University of Massachusetts Dartmouth
† kwage@gmu.edu
Electrical and Computer Engineering Department
George Mason University

ABSTRACT

Co-prime sensor arrays (CSAs) interleave two uniform linear subarrays that are undersampled by co-prime factors. The resulting non-uniform array requires far fewer sensors to match the spatial resolution of a fully populated ULA of the same aperture. Choosing the co-prime undersampling factors as close to equal as possible minimizes the number of sensors in the CSA. However, the peak side lobe of the CSA is higher than the peak side lobe of the equivalent full uniform linear array (ULA). Increasing the number of sensors in the CSA subarrays by half while maintaining the interelement spacing gurarantees that the CSA peak side lobe is less than that of the full aperture ULA when both arrays use rectangular windows.

Index Terms— Co-prime arrays, sampling, beamforming, uniform linear array

1. INTRODUCTION

The performance of a linear array in the detection and direction of arrival estimation of a narrowband signal is highly dictated by the physical aperture of the array and the interelement spacing between the array elements. Improving the resolution of the array requires increasing the array aperture while keeping the interelement spacing less than half-wavelength to avoid spatial aliasing or grating lobes. For a given array aperture, reducing the number of elements translates into reduced acquisition and maintenance cost, increased system reliability and decreased system hardware complexity. Several techniques exist in the literature to minimize the number of sensors for a given aperture [1], [2], [3], [4], [5], [6], [7], [8], [9]. Pal and Vaidyanathan introduced the concept of using nested ULAs that can provide far more degrees of freedom than the number of sensors in the array [1]. Unequally spaced, broad-band antenna arrays that require fewer elements for comparable beamwidth were discussed in [2]. Unz found the relationship between the arbitrarily distributed elements of linear arrays and the radiation patterns of the linear arrays [3]. Ishimaru proposed a novel method to design non-uniform arrays with desired radiation patterns in [4]. Based on [4], a method for designing thinned non-uniform arrays with required beamwidths was presented in [5]. Moffet introduced the minimum redundancy linear arrays that achieve maximum resolution for a given number of sensors by removing the redundant interelement spacings in the arrays [6]. Steinberg compared various thinned aperiodic arrays to a set of random arrays in [7]. Such techniques often lead to undesirable non-uniform sensor locations and eccentric side lobe properties for the array beam pattern. The co-prime sensing technique recently proposed by Vaidyanathan and Pal [10] combines two ULAs to produce a non-uniform array requiring substantially fewer sensors than a ULA spanning the same aperture. The uniform linear geometry of the two constituent arrays makes CSAs easier to construct and maintain than many other non-uniform array design techniques. Moreover, the side lobe properties of CSAs are predictable and manageable.

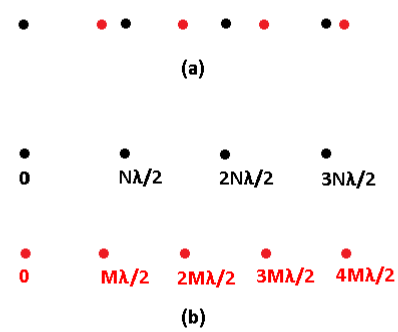

Fig. 1: (a) A co-prime sensor array (b) Separating a co-prime sensor array into its two uniform linear subarrays

CSAs interleave two undersampled ULAs, referred to as the CSA subarrays in the sequel, to produce a non-uniform linear array. Figure 1(a) illustrates an example CSA generated by combining a subarray with M elements and $N\lambda/2$ interelement spacing (black dots) and the other subarray with N elements and $M\lambda/2$ interelement spacing (red dots), with $(M, N) = (4, 5)$. Each subarray's sensors are indicated by different colors (black and red) with the first sensor at 0 shared by both subarrays. Figure 1(b) illustrates the CSA decomposed into the two uniform linear subarrays. Figure 1 and the rest of the paper assume that $N > M$ without loss of generality. The spatial undersampling factors M and N must be co-prime to avoid grating lobes in the CSA beam pattern, as discussed below.

CSAs perform conventional beamforming on each uniform subarray separately, then multiply the two resulting beam patterns to obtain a total beam pattern. The resulting product beam pattern has

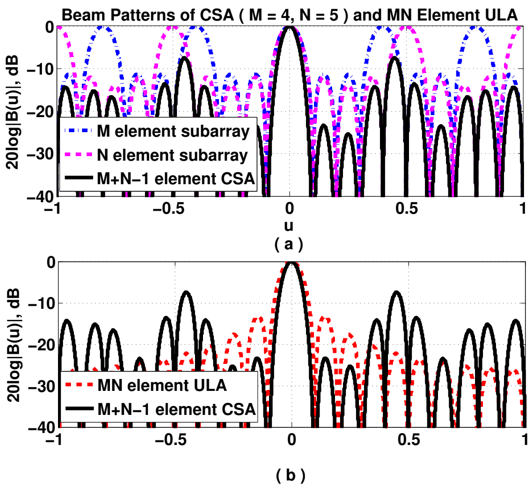

Fig. 2: (a) Formation of the beam pattern of a CSA from the beam patterns of the ULAs (b) Comparison of the beam patterns of a CSA and its equivalent full ULA

resolution equivalent to a fully sampled ULA with MN elements. More importantly, when M and N are co-prime, the grating lobes of the two subarrays appear in different locations. So, the resulting product beam pattern (solid black line in Figure 2(a)) does not have grating lobes [10]. This decrease from the MN elements of the fully sampled ULA to the $M + N - 1$ elements of the CSA represents a significant savings in system complexity, cost and computational requirements.

The beam patterns of the two conventionally beamformed subarrays using rectangular windows (or shading) are described by the equations

$$B_{M,N}(u) = \frac{1}{M} \frac{\sin(\frac{\pi MN}{2}u)}{\sin(\frac{\pi N}{2}u)} \tag{1}$$

$$B_{N,M}(u) = \frac{1}{N} \frac{\sin(\frac{\pi NM}{2}u)}{\sin(\frac{\pi M}{2}u)}, \tag{2}$$

where $u = \cos(\theta)$ is the directional cosine and θ is the direction of arrival with respect to the CSA axis [8]. Figure 2(a) shows example subarray beam patterns (blue dash-dot and magenta dash lines) for the CSA shown in Figure 1. Both subarrays are steered to broadside ($u = \cos(\pi/2) = 0$). Figure 2(b) compares the beam patterns of an $M + N - 1$ element CSA and an MN element ULA. Though the two beam patterns achieve the same resolution, the peak side lobe level of the CSA beam pattern is larger than the peak side lobe level of the MN element ULA. Vaidyanathan and Pal [10] suggest that the high side lobes of the CSA can be reduced by extending each CSA subarray to reduce the grating lobe widths of the subarray beam patterns. Reducing the grating lobe widths minimizes the overlap between two grating lobes, reducing the overall CSA peak side lobe level. However, Vaidyanathan and Pal do not provide any guidelines on how many additional sensors are required. Also, they do not suggest how to choose the co-prime factors M and N when several choices are available.

This paper focuses on two issues that are not addressed in [10]: How can we choose the co-prime undersampling factors M and N for a given aperture when different options are available? How many sensors should we add to each subarray to achieve peak side lobe attenuation comparable to the equivalent MN element ULA?

2. CO-PRIME FACTORS

To obtain the resolution of an L element ULA with a CSA, L has to be factored into two co-prime integers M and N. For some L, several choices of co-prime pairs are available. For example, to obtain the resolution of a 60 element ULA, a CSA can choose any of the following, $(M, N) = (2, 30)$, $(M, N) = (3, 20)$, $(M, N) = (4, 15)$ or $(M, N) = (5, 12)$. The optimal co-prime pair (M, N) is the one that minimizes the total number of sensors $M + N$ since this reduces acquisition cost, maintenance cost, system weight and hardware complexity. This is a straightforward constrained optimization problem:

$$\begin{aligned} Minimize \quad & M + N \\ subject \quad to \quad & MN = L \\ & M > 0 \\ & N > 0 \end{aligned} \tag{3}$$

The optimal values of M and N as given by Lagrange's multiplier optimization are $M = N = \sqrt{L}$. The co-primality requirement between M and N makes this choice invalid, but the solution implies that the co-prime pair M and N closest to equal ($\sqrt{L}$) are the best choice. So, the optimal pair for $L = 60$ is $(M, N) = (5, 12)$. If the resolution of a ULA with slightly fewer than L elements is acceptable, M and N with a difference of 1 can be chosen to save a few more sensors. For example, in the previous example, $(7, 8)$ can be chosen instead of $(5, 12)$ saving two more sensors (reducing the number of sensors required by almost 12%) at a cost of less than 7% in resolution relative to the $(5, 12)$ CSA. Figure 3 depicts the effect of choosing different co-prime factors for the integer $L = 210$. (Note that 210 is the smallest integer that can be factored into co-prime pairs in 7 ways.) The vertical axis represents the total number of sensors required by a CSA matching the corresponding ULA performance in resolution and peak side lobe level. The horizontal axis represents the different co-prime factors for $L = 210$, progressing from most to least commensurate. The plot shows that in general, the total number of sensors in the extended CSA increases as M and N become less equal. For the Dolph-Chebyshev and Hanning shadings, the trend follows strictly. For rectangular shading, there are some fluctuations but the general trend still holds as M and N grow less equal.

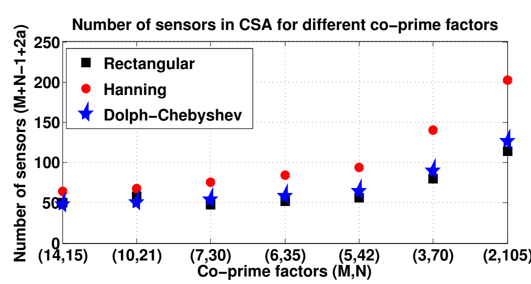

Fig. 3: Comparison of different co-prime factors of 210

The following sections will assume that the CSA has been optimized to make the total number of sensors minimum which in general means $N = M + 1$.

3. EXTENSION FACTOR OF THE CSA SUBARRAYS

In a CSA with co-prime factors M and N, the grating lobes of the M element subarray are located at integer multiples of $2/N$ in $u = \cos(\theta)$ and the grating lobes of the N element subarray are located at integer multiples of $2/M$ in u. When $N = M + 1$, the first grating lobes of the two subarrays are exactly $2/(MN)$ units apart in u. The intersection of these adjacent grating lobes gives rise to the peak side lobe of the CSA beam pattern as shown in Figure 2(a). As also shown in Figure 2(b), the peak side lobe level of the CSA is higher than the peak side lobe of the corresponding ULA. To make the peak side lobe level of the CSA smaller, the overlap between the two adjacent grating lobes must be be reduced. Extending each subarray by an additional number of sensors (a) while keeping the same interelement spacing increases the aperture of the subarrays and the overall CSA. The increased aperture reduces both the main lobe and grating lobe widths of the subarrays. In contrast, the locations of the grating lobes of the subarrays do not change since their locations are determined by the interelement spacing which is not changing. Reducing the grating lobe widths while maintaining the separation between them reduces the overlap of the adjacent grating lobes, and consequently the peak side lobe of the product beam pattern [10]. The extended CSA will result in a beam pattern that has higher resolution than an MN element ULA. The resolution of the extended CSA can be compared to the resolution of a full ULA with $(N + a)M$ elements (assuming $N > M$).

There are two mechanisms by which the extended subarrays' beam patterns combine to generate the peak side lobe of the CSA. For the basic CSA, the peak side lobe is due to the intersection of the two adjacent grating lobes (as noted above). As sensors are added, there is a transition to a peak side lobe generated by the intersection of one grating lobe and one side lobe. The type of shading determines how many additional sensors are required to trigger the transition from one mechanism of peak side lobe generation to the other.

For shadings like rectangular where Fourier transform of the shading window has decreasing side lobes, the peak side lobe in CSA can be due to the intersection of a grating lobe from one of the subarrays and a side lobe from another subarray even for a relatively small number of additional sensors. Figure 4(a) illustrates that the overlap of a grating lobe from one subarray with the first side lobe from the second subarray creates the peak side lobe.

For rectangular shading, the beam pattern of the $M + a$ element subarray with $N\lambda/2$ interelement spacing is

$$B_{M+a,N} = \frac{1}{M+a} \frac{\sin(\frac{\pi(M+a)Nu}{2})}{\sin(\frac{\pi Nu}{2})}. \tag{4}$$

The side lobes occur approximately at the places where the numerator of the beam pattern is 1, i.e. $u = \pm(2m + 1)/((M + a)N)$, where m is an integer. Hence, the side lobe levels are approximately given by $-20 \log |(M+a) \sin(0.5(2m+1)\pi/(M+a))|$. When the number of sensors is large, the peak side lobe level is approximately -13.5 dB [8]. When a is large enough such that the peak side lobe is formed by the intersection of one grating lobe and one first side lobe, the CSA peak side lobe equals the height of the first side lobe of a subarray (approximately -13.5 dB) which in turn is almost equal to the peak side lobe of the corresponding full ULA.

The number of additional sensors a that will guarantee that the peak side lobe level of the CSA for rectangular shading is below the peak side lobe level of the equivalent ULA can be found analytically. The first grating lobe of the $N + a$ element subarray of a CSA is at $2/M$ and the first grating lobe of the $M + a$ element subarray is at $2/N$. The first side lobe of the $M + a$ element subarray appears at $3/((M + a)N)$ units from its grating lobe. Hence, the first side lobe of the $M + a$ element subarray aligns under the first grating lobe of the $N + a$ element subarray when

$$\frac{2}{N} + \frac{3}{(M + a)N} = \frac{2}{M}. \tag{5}$$

Solving the above equation for a gives us $a = 0.5M$ for $N = M + 1$. Similarly, the first side lobe of the $N + a$ element subarray aligns under the first grating lobe of the $M + a$ element subarray when $a = 0.5N$.

At the center of the two adjacent grating lobes ($u_0 = 1/M + 1/N$) which is approximately where the two grating lobes intersect,

$$B_{M+a,N}(u_0) = \frac{\sin(0.75\pi(2M + 1))}{1.5M \sin(0.5\pi(2M + 1)/M)} \tag{6}$$

For $M > 1$, $20(\log(B_{M+a,N}(u_0)B_{N+a,M}(u_0)) < -19$ dB. Hence, when $a \geq 0.5M$, the intersection of the grating lobes is less than the peak side lobe of one subarray, guaranteeing that the peak CSA side lobe is generated by the alignment of a side lobe with a grating lobe. Hence, for large a, the largest possible peak side lobe of CSA occurs when the first side lobe of the $M + a$ element subarray comes exactly under the grating lobe of the $N + a$ element subarray. Therefore, a sufficient condition for the peak side lobe of CSA to be less than the peak side lobe of an equivalent full ULA is $a \geq \lceil 0.5M \rceil$. However, this is not a necessary condition. For certain cases, the CSA may equal the peak side lobe of the full ULA for values of $a < M/2$. Similar phenomena exist for windowed FIR filter design, where the filter length required for a Kaiser window may deviate slightly from the design equation guidelines [11].

For an equiripple window like Dolph-Chebyshev, if the side lobes are larger than the peak side lobe of a rectangular window, the main lobe and grating lobe widths are wider than that of the rectangular window. Therefore, the overlap of the two adjacent grating lobes persists to larger values of a. Increasing a decreases the peak side lobe level of the CSA, but for a certain value of a,

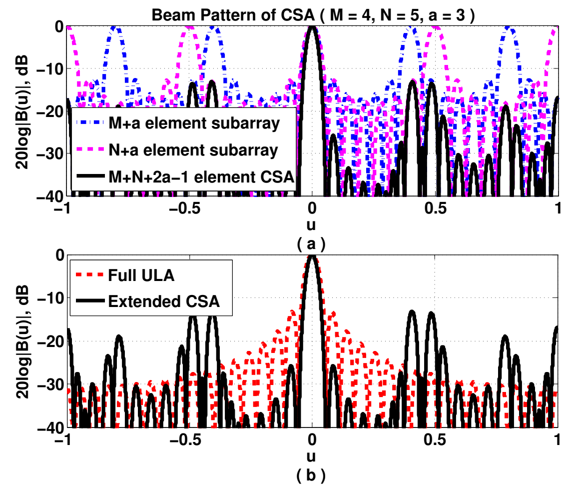

Fig. 4: Comparison of the beam patterns of an extended CSA and a full ULA with an equivalent resolution

the overlap of the two adjacent grating lobes will result in the peak side lobe level that is equal to or less than the side lobe level of one subarray. Increasing a beyond that value cannot reduce the peak side lobe level of the CSA. The peak side lobe remains equal to the side lobe of a subarray. However, the location of peak side lobe can vary abruptly. Figure 5(a) shows that for $(M, N) = (4, 5)$, the peak side lobe is still due to the intersection of two grating lobes even for a as large as 5. But for $a = 6$ or more, the peak side lobe is due to one grating lobe and one side lobe. For $a = 9$, the peak side lobe location shifts substantially as the peak side lobe near $u = 1$ is in fact about 0.3 dB higher than the side lobes created near the first pair of grating lobes at $u = 0.4$ and 0.5 as shown in Figure 5(b).

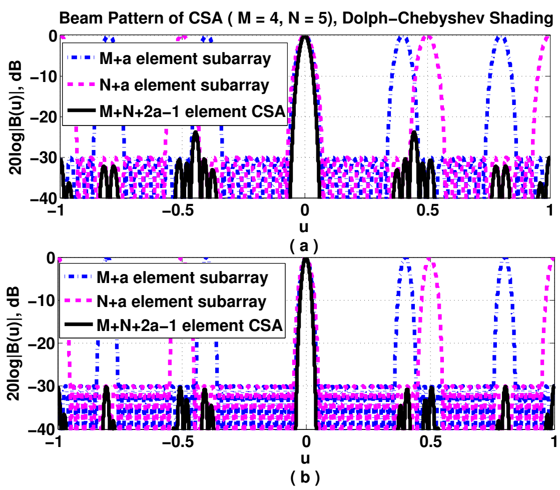

Fig. 5: Extended CSA with Dolph-Chebyshev shading (a) $(M, N, a) = (4, 5, 5)$ (b) $(M, N, a) = (4, 5, 9)$

For windows whose side lobes attenuate away from the main lobe, the peak side lobe of a CSA can be made even smaller than the corresponding full ULA with the same window. Continuing to increase the number of sensors in the CSA further reduces the widths of the grating lobes and side lobes, while the grating lobe locations for the subarrays remain fixed. Consequently, the peak side lobe eventually is created by the alignment of the second side lobe of one subarray with the grating lobe of the other subarray. This product is less than the peak side lobe of the full ULA. The process continues as more sensors are included, aligning the third and subsequent side lobes of one subarray beam pattern below the grating lobe of the other array. However, for equiripple shadings like Dolph-Chebyshev, the peak side lobe cannot be reduced beyond the peak side lobe of one subarray because the subsequent sidelobes do not attenuate.

4. CONCLUSION

This paper shows that the optimum co-prime factors in a CSA are the ones as close to equal as possible for a given aperture. The paper discusses the location and formation of the peak side lobe in an extended CSA and derives a sufficient condition on the extension factor for the peak side lobe of the CSA to be less than that of full ULA when the array shading is rectangular.

In the interest of brevity and simplicity, this paper focused on peak side lobe results for the case $N = M + 1$ with the rectangular window, but the same approach can be extended to other co-prime pairs and array shading windows.

5. REFERENCES

[1] P. Pal and P. P. Vaidyanathan, "Nested arrays: A novel approach to array processing with enhanced degrees of freedom," *IEEE Trans. Signal Process.,* vol. 58, no. 8, pp. 4167-4181, Aug. 2010.

[2] D. D. King, R. F. Packard and R. K. Thomas, "Unequally spaced broad-band antenna arrays," *IRE Trans. Antennas Propag.,* vol. AP-8, pp. 380-385, July 1960.

[3] H. Unz, "Linear arrays with arbitrarily distributed elements," *IRE Trans. Antennas Propag.,* vol. AP-8, pp. 222-223, March 1960.

[4] A. Ishimaru, "Theory of unequally spaced arrays," *IRE Trans. Antennas Propag.,* vol. AP-10, pp. 691-702, November 1962.

[5] A. Ishimaru and Y. S. Chen, "Thinning and broadbanding antenna arrays by unequal spacings," *IRE Trans. Antennas Propag.,* vol. AP-13, pp. 34-42, January 1965.

[6] A. Moffet, "Minimum-redundancy linear arrays," *IEEE Trans. Antennas Propag.,* vol. 16, pp, 172-175, Mar. 1968.

[7] B. D. Steinberg, "Comparison between the peak sidelobe of the random array and algorithmically designed aperiodic arrays," *IEEE Trans. Antennas Propag.,* May 1973

[8] H. L. Van Trees, *Optimum Array Processing: Part IV of Detection, Estimation and Modulation Theory.* New York: Wiley-Interscience, 2002.

[9] D. H. Johnson and D. E. Dudgeon, *Array Signal Processing: Concepts and Techniques.* Upper Saddle River, NJ: Prentice-Hall, 1993.

[10] P. P. Vaidyanathan and P. Pal, "Sparse sensing with coprime samplers and arrays," *IEEE Trans. Signal Process.,* vol. 59, no. 2, pp. 573-586, Feb. 2011.

[11] A. V. Oppenheim and R. W. Schafer, *Discrete Time Signal Processing.* Englewood Cliffs, NJ: Prentice-Hall, 1999.